Modified Combline Filter for A Compact Size

By Kai Wang

Under the Supervision of Professor In-ho Kang

Department of Radio Sciences and Engineering

In the Graduate School

of

Korea Maritime University

June 2006

Modified Combline Filter for A Compact Size

By Kai Wang

Under the Supervision of Professor In-ho Kang

Department of Radio Sciences and Engineering

In the Graduate School

of

Korea Maritime University

June 2006

Modified Combline Filter for A Compact Size

By Kai Wang

Here is approved that this is the thesis

submitted in partial satisfaction of the requirements for degree of

MASTER

in Engineering in the Graduate School of

Korea Maritime University.

Approved: Prof. Young Yun

Prof. Dongkook Park

Prof. In-ho Kang

Committee in Charge

Contents

Nomenclature

f	:	Frequency
f_0	:	Center frequency
Q	:	Quality factor
SIR	:	Step impedance filter
MMIC	:	Monolithic microwave integrated circuit
MIM	:	Metal-Insulator-Metal
Z_0	:	Characteristic Impedance
Z_{0e}	:	Even mode impedance
Z_{0o}	:	Odd mode impedance
Y	:	Characteristic admittance
Θ	:	Electrical length
$S_{ij}(i = j)$	:	Reflection coefficient
$S_{ij}(i \neq j)$	:	Transmission coefficient
K	:	Coupling coefficient

List of Tables

List of Figures

Abstract

Bandpass filters are widely used in microwave systems. And miniaturized bandpass filters are required to reduce the cost of a wireless communication system. Therefore, many prototypes have been studied to meet this requirement. The conventional comb-line filter is one of the so many types of proposed size-reduced filters. In this thesis, we propose a modified comb-line filter using a combination of end shorted parallel coupled lines and lumped capacitors. Using the above structure, the electrical length of the parallel coupled lines in the modified comb-line filter, which determines the size of a comb-line filter, can be reduced to even a few degrees, resulting in a much smaller circuit area. Inter-stage connecting lines have been added to connect the neighboring resonators for the suppression of unwanted coupling. The designed comb-line filter also shows a wide upper stopband. Design equations and method will be fully explained in this thesis. Measured results of a fabricated filter centered at 400 MHz show good agreement with the theoretical predications.

Chapter 1 Introduction

Compact microwave bandpass filters are intensely required in mobile communication systems. This necessity has been attracting great attention in microwave community and many innovative filter prototypes have already been proposed. One intensely studied miniaturized type is step impedance filters (SIR), among which the quarter-wavelength type SIR is the most attractive. [1] Slow-wave resonator filter [2] represents another approach in reducing the size of band-pass filters by making use of the slow-wave effect in periodic structures. Each of the above structures can miniaturize a band-pass filter to some extent, but still these filters take up a pretty large circuit area, especially at lower microwave frequency band.

In this thesis we introduce a modified comb-line filter using end shorted coupled lines and lumped capacitors. The electrical length of the parallel coupled lines is just a few degrees, making the total size of the proposed filter very small even at a low frequency band. The spurious passband, an annoying disadvantage of many microstrip filters, has also been brought to well control using the proposed structure, and the reasons will be given in details in later chapters.

1.1 An introduction to Comb-line filters

The conventional comb-line filter will be briefly introduced in this section, as it will be compared with the proposed modified one in many ways in this paper [3]. Shown in Fig. 1.1 is a traditional comb-line bandpass filter in stripline form. The resonators consist of line elements which are shorted-circuited at one end, with a lumped capacitance C_j^s between the other end of each resonator line element and ground. In this figure, Line 1 to n, along with their associated lumped capacitances C_1^s to C_n^s comprise resonators, while line 0 to n+1 are not resonators but simply part of impedance-transforming sections at the ends. Coupling between resonators is achieved in this type of filter by way of the fringing fields between resonators lines. With the lumped capacitors, the resonators lines will be less that a quarter of wavelength at resonance. If the capacitors were not present, the resonator lines would be a full quarter-wavelength long at resonance and the structure would have no pass band at all. For the reasons above, it is usually desirable to make the capacitances C in this type of filter sufficiently large that the resonator lines will be $\lambda_0 / 8$ or less, long at resonance. Besides having efficient coupling between resonators, the resulting filter will be quite small.

One disadvantage of the microstrip parallel coupled filter is that the first spurious pass-band of this type of filter appears at twice of the basic pass-band frequency ($2 f_0$). This is because the even-mode phase velocity is always slower than that of the odd mode because of

the inhomogeneous medium of microstrip structure. The unequal modal phase velocities at $2\,f_0$ cause the first spurious pass-band. As for comb-line filters, the second pass band occurs when the resonator line elements are somewhat over a half-wavelength long, so if the resonator line elements are $\lambda_0/8$ long at the primary pass band, the second pass band will be centered at somewhat over four times the frequency of the center of the first pass band. If the resonator line elements are made to be less than $\lambda_0/8$ long at the primary pass band, the second pass band will be even further removed. Thus, comb-line filters also lend themselves to achieving very broad stop bands above their primary pass bands.

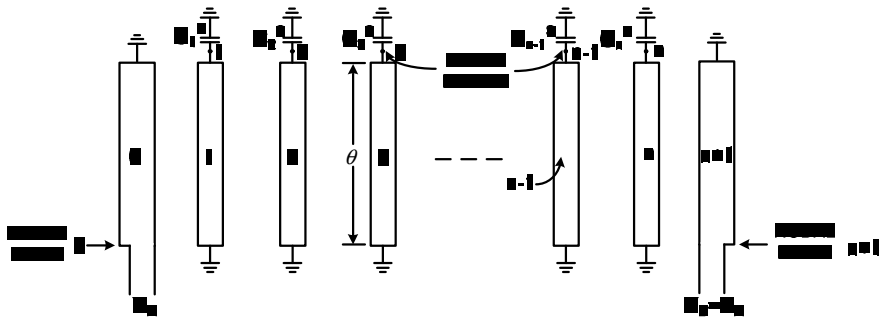

Fig. 1.1 The model of the conventional comb-line filter.

1.2 Research Contents

Chapter 1 depicts the background and purpose of this work and briefly introduces the outline of the thesis.

Chapter2 focuses on the miniaturization of quarter-wavelength transmission line. The theoretical analysis, circuit design equations are presented in this chapter.

Chapter 3 introduces the design theory of the bandpass filters based on a generalized bandpass filter structure. The theoretical analysis and detailed design method are explained here, together with the simulated results through Advanced Design System (ADS).

Chapter 4 shows the whole fabrication process, from HFSS simulation to measurement. Analyses of the measured results also take up some space here. The reasons for the differences between measured and simulated results are explained.

Chapter 5 is the conclusion of this research work, followed by the future research plan.

Chapter 2 Miniaturization of the Quarter-wavelength Transmission Line

2.1 Introduction

The quarter-wavelength transmission line has been playing a very important role in many microwave circuits, functioning as impedance transformers, phase inverters and so on. However, in many cases, this quarter-wavelength is too large to be compatible with other parts of microwave systems. This problem has become even severe in monolithic microwave integrated circuit (MMIC), since a large circuit area always results in a high chip cost. Hirota proposed a size-reduction method which utilizes combinations of short high-impedance transmission lines and shunt lumped capacitors [4], as shown in Fig.2.1. With the help of lumped capacitors, a λ/4 transmission line can be made to be as short as λ/12. Therefore, this size-reduction method has been employed in various kinds of microwave circuits where quarter-wavelength transmission line exists. However, an obvious disadvantage of this method is that the impedance of the shortened transmission line $Z_0^{'}$ increases rapidly as its electrical length decreases. Usually the length of the shortened transmission line could be no smaller than λ/12, because the large impedance (over 100 Ohm) inevitably results in a very thin microstrip line that is hard to fabricate using the general etching method.

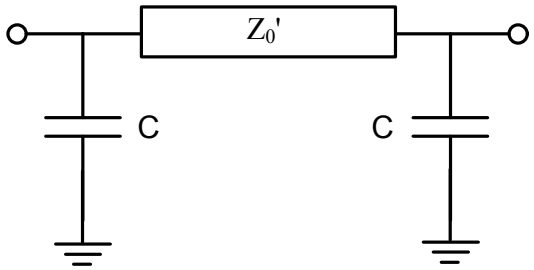

Fig. 2.1 Size-reduced quarter-wavelength transmission line using shortened transmission line and lumped capacitors.

Another approach to miniaturize the quarter-wavelength transmission line is to use lumped inductors and capacitors, as shown in Fig.2.2. The lumped elements do take up very small space. However, the design of lumped-element circuits must be somewhat empirical, and it needs precise inductor models based on careful measurements of test elements. This inductor can be realized with air-wound coils, but such coils must be space-wound with gaps between turns, resulting in wide variations in their inductance value [5]. Spiral inductors represent another possible compromise, although their quality factor (Q) is often sacrificed to adequate inductance. Equivalent lumped-element models for spiral inductors have been obtained from two-port S-parameter measurements. There models do not lend themselves readily to design applications because their elements are difficult to evaluate in advance [6], [7], [8]. Gupta presented a quasi-lumped-element branch-line coupler, which uses lumped capacitors and short-circuited transmission lines as inductors, but the resulting design is inconvenient to fabricate [9].

Instead of continuing the search for applicable inductors, we propose in this paper a method to replace the inductor shown in Fig.2.2, by using a combination of end shorted coupled lines and lumped capacitors. With this method, the quarter-wavelength transmission line can be made to be as short as a few degrees, resulting in a very compact circuit. The impact related to the imprecise inductor value has been eliminated since only lumped inductors are utilized.

2.2 Size-reducing method of the λ/4 transmission line

The size-reduction of quarter-wavelength transmission line is done here through a series of equivalent circuit transformation. As mentioned above, the quarter-wavelength transmission line can be equated to a combination of lumped inductor and capacitors, as illustrated in Fig.2.2 (a) and (b). The value of the capacitors is needed for further study, and it can be obtained by comparing the ABCD matrices of the two circuits in Fig. 2.2, as given in (2.1) and (2.2), respectively:

$$\begin{pmatrix} A & B \\ C & D \end{pmatrix} = \begin{pmatrix} 0 & jZ_0 \\ j/Z_0 & 0 \end{pmatrix} \tag{2.1}$$

$$\begin{pmatrix} A' & B' \\ C' & D' \end{pmatrix} = \begin{pmatrix} 1 & 0 \\ j\omega C_1 & 1 \end{pmatrix} \begin{pmatrix} 1 & j\omega L \\ 0 & 1 \end{pmatrix} \begin{pmatrix} 1 & 0 \\ j\omega C_1 & 1 \end{pmatrix}$$

$$= \begin{pmatrix} 1-\omega^2 C_1 L & j\omega L \\ j\omega L + j\omega C_1 - j\omega^3 C_1^{\,2} L & 1-\omega^2 C_1 L \end{pmatrix} \tag{2.2}$$

By making $1-\omega^2 C_1 L = 0$ and $jZ_0 = j\omega L$, we can get the value of C_1 as,

$$C_1 = \frac{1}{\omega Z_0} \tag{2.3}$$

where Z_0 is the characteristic impedance of the quarter-wavelength transmission line and ω the angular frequency.

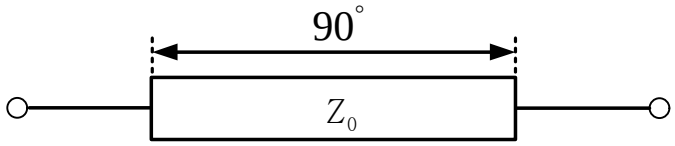

(a)

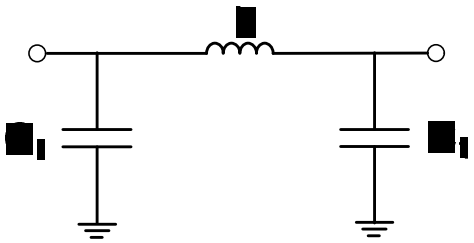

(b)

Fig. 2.2 The quarter-wave transmission line: (a) distributed and (b) equivalent lumped elements.

Now to replace the lumped inductor, we first add two artificial LC resonances consisting of C_0 and L_0 at each side of the lumped inductor, as shown in Fig. 2.3. The ABCD matrix of the dotted PI network is given below in (2.4):

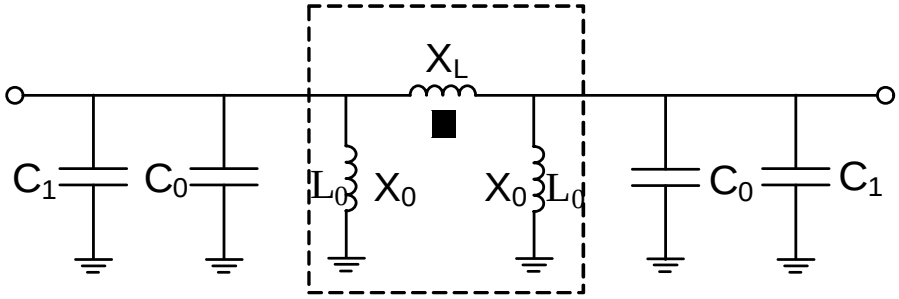

Fig. 2.3 Equivalent circuit of a λ/4 transmission line with artificial resonance circuits inserted.

$$\begin{pmatrix} A & B \\ C & D \end{pmatrix} = \begin{pmatrix} 1+\frac{X_0}{X_L} & \frac{1}{X_L} \\ 2X_0+\frac{X_0^{\,2}}{X_L} & 1+\frac{X_0}{X_L} \end{pmatrix} \qquad (2.4)$$

where

X_0 = shunt impedance in the PI network;

X_L = series impedance in the PI network.

Before moving forward with our theory, let's firstly look at Fig.2.4, where an end-shorted coupled line pair and its equivalent PI network are offered. (A180° phase shift does exist between (a) and (b), but will be proved to be ignorable in designing the proposed filter) [10]. The ABCD matrix of this PI network is:

$$\begin{pmatrix} A' & B' \\ C' & D' \end{pmatrix} = \begin{pmatrix} 1+\dfrac{Z_{0e}\tan\theta}{\dfrac{2Z_{0o}Z_{0e}}{Z_{0e}-Z_{0o}}\tan\theta} & \dfrac{1}{j\dfrac{2Z_{0o}Z_{0e}}{Z_{0e}-Z_{0o}}\tan\theta} \\ 2jZ_{0e}\tan\theta+\dfrac{jZ_{0e}{}^2\tan^2\theta}{\dfrac{2Z_{0o}Z_{0e}}{Z_{0e}-Z_{0o}}\tan\theta} & 1+\dfrac{Z_{0e}\tan\theta}{\dfrac{2Z_{0o}Z_{0e}}{Z_{0e}-Z_{0o}}\tan\theta} \end{pmatrix} \quad (2.5)$$

where

Z_{0e}, Z_{0o} = even and odd mode impedances of the end shorted coupled lines, respectively

θ = electrical length of the miniaturized transmission line.

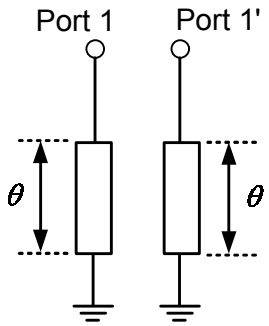

(a)

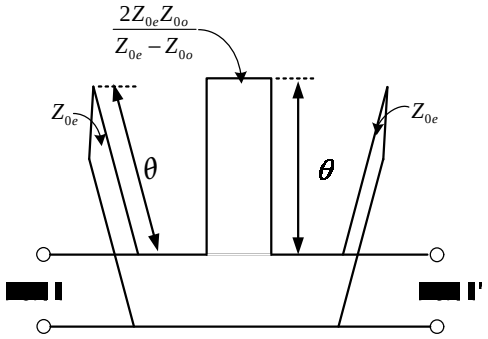

(b)

Fig. 2.4 The end shorted coupled lines (a) and the equivalent PI network (b).

According to (2.4) and (2.5), if the following two equations:

$$1+\frac{X_0}{X_L}=1+\frac{Z_{0e}\tan\theta}{\frac{2Z_{0o}Z_{0e}}{Z_{0e}-Z_{0o}}\tan\theta}, \tag{2.6.1}$$

$$\frac{1}{X_L}=\frac{1}{j\frac{2Z_{0o}Z_{0e}}{Z_{0e}-Z_{0o}}\tan\theta} \tag{2.6.2}$$

are satisfied, we can see that the PI network in the dotted box in Fig.2.3 would be equal to the Pi network shown in Fig. 2.4 (b). And by simplifying (2.6.1) and (2.6.2) we get :

$$X_0 = Z_{0e}\tan\theta \tag{2.7.1}$$

$$X_L=\frac{2Z_{0e}Z_{0o}}{Z_{0e}-Z_{0o}}\tan\theta \tag{2.7.2}$$

Based on (2.7.1) and (2.7.2), we can replace the circuits in the dotted box in Fig.2.3 with the end shorted coupled lines in Fig. 2.4 (b). The resultant circuit is illustrated in Fig.2.5. From (2.7.1), the value of C_0 is:

$$C_0=\frac{1}{\omega Z_{0e}\tan\theta} \tag{2.8}$$

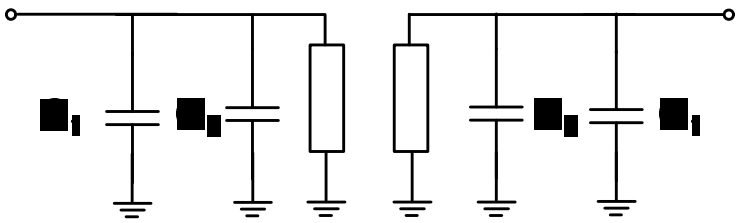

Fig. 2.5 The miniaturized quarter-wavelength line with end shorted coupled lines and lumped capacitors.

In the following simulation and fabrication, we always use one capacitor C that is equal to the sum of C_0 and C_1, and we get the simplified circuit of the miniaturized quarter-wavelength transmission line, as expressed in Fig. 2.6. Equation (9) will be used in this paper to calculate the capacitor C.

$$\begin{aligned} C &= C_0 + C_1 \\ &= \frac{1}{\omega Z_0} + \frac{1}{\omega Z_{0e} \tan\theta} \end{aligned} \tag{2.9}$$

Where Z_0 is the characteristic impedance of the quarter-wavelength microstrip transmission line.

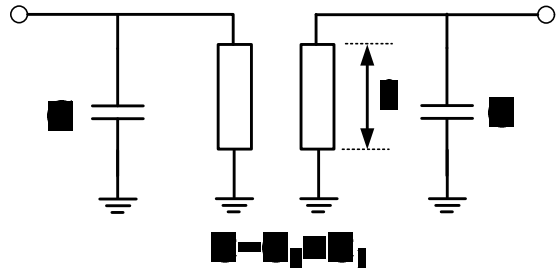

Fig.2.6 Miniaturized quarter-wavelength transmission line with the lumped capacitor C.

If we define $Z^{'} = \frac{2Z_{0e}Z_{0o}}{Z_{0e} - Z_{0o}}$ as the characteristic impedance of the end shorted coupled lines, then with (2.7.2) we get:

$$Z^{'} = X_L \cot\theta \tag{2.10}$$

From (2.1) and (2.2), we can get $X_L = Z_0$, so (2.10) can be re-expressed as:

$$\begin{aligned} Z^{'} &= \frac{2Z_{0e}Z_{0o}}{Z_{0e} - Z_{0o}} \\ &= \frac{Z_0}{\tan\theta} \end{aligned} \tag{2.11}$$

The following table lists a set of data calculated through (2.9) and (2.11) for the interested readers. In the table, a quarter-wavelength transmission line working has been miniaturized to different length from 1 degree to 12 degree. By fixing Z_{0e} at 70 Ohm, we can get Z_{0o}.The value of C is calculated supposing the angular frequency ω is 1 GHz.

Table 2.1 A set of design data at 1 GHz for reference.

θ (Deg.)	$Z^{'}(\Omega)$	Z_{0e} (Ω)	Z_{0o} (Ω)	C (pF)
1	2864.50	70.00	66.71	133.50
2	1431.81	70.00	63.77	68.30
3	954.06	70.00	61.04	46.59
4	715.03	70.00	58.50	32.53
5	571.50	70.00	56.23	29.18
7	407.22	70.00	52.09	21.71
8	355.77	70.00	50.23	19.37
9	315.69	70.00	48.49	19.54
10	283.56	70.00	46.86	16.08
11	257.23	70.00	45.33	14.88
12	235.23	70.00	43.88	13.88

Chapter 3 Bandpass Filter Design Theory

3.1 Introduction

The filter to be studied here is based on a generalized bandpass filter model provided by [11], as shown in Fig.3.1, where $B_n(\omega)$ (n=1~N) represents resonant circuits and J_{0n} (n=1~N) admittance inverters. An idealized admittance inverter operates like a quarter-wavelength line of characteristic admittance J at all frequencies. Thus, if an admittance Y_b is attached at one end, the admittance Y_a seen looking in the other end is:

$$Y_a = \frac{J^2}{Y_b} \tag{3.1}$$

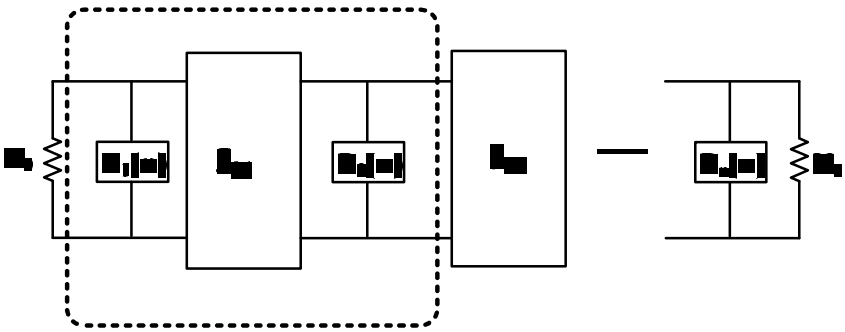

Fig. 3.1 A generalized, bandpass filter circuit using admittance inverters.

There are numerous circuits that operate as inverters. One of the simplest forms among these inverters is a quarter-wavelength transmission line. The admittance inverter parameter of the quarter-wavelength transmission line inverter will be $J = Y_0$, where Y_0 is the characteristic admittance of the transmission line. Although

the inverter properties are relatively narrow-band in nature, this quarter-wavelength line can be used without any problem as an admittance inverter in our proposed narrow band filters.

3.2 Size-reduced Bandpass filter

We here employ the above discussed quarter-wavelength transmission line inverters in our proposed filter. Based on the bandpass filter model in Fig.3.1, a one-stage bandpass filter is proposed in Fig.3.2, where two LC resonant circuits functions as $B_1(\omega)$ and $B_2(\omega)$. To get a compact filter, the λ/4 transmission line admittance inverter is miniaturized using the method discussed above, resulting in the circuit in Fig.3.2 (b). Here we should mention that the two inductors in the resonant circuits at each side of the admittance inverter in Fig. 3.2 have been replaced by the coupled lines as discussed in last chapter. The two LC circuits are hidden but still functions as resonators, which has reduced the number of needed lumped elements in the proposed filter. Therefore, the circuit in Fig.2.6 can be used as the finally miniaturized one-stage bandpass filter.

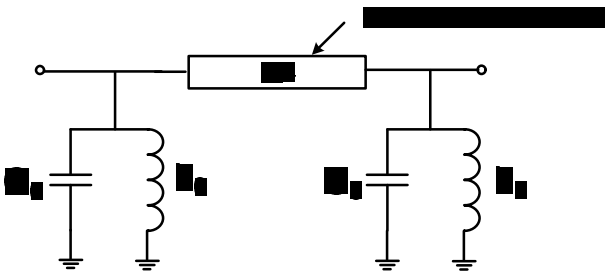

(a)

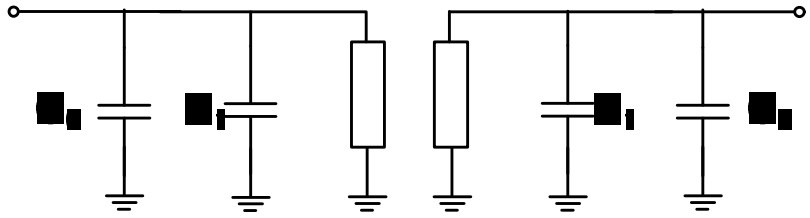

(b)

Fig. 3.2 A one-stage bandpass filter based on the generalized filter model (a) and its miniaturized form (b).

Fig.3.3 gives the ADS model of the proposed size-reduced one- and two-stage filters. A three-stage filter can be realized simply by connecting one more stage and is therefore omitted here. Two- and three-stage filters certainly have sharper skirt characteristics, but in fabrication the use of many stages usually leads to a relatively larger insertion loss. Therefore, a compromise sometimes should be made between sharp skirt characteristics and small insertion loss. The simulation results of the 1-, 2- and 3-stage of the proposed bandpass filters have been given Fig.3.4 to confirm the discussion in this paragraph, where the electrical length of the coupled lines is chosen to be 7 Degree.

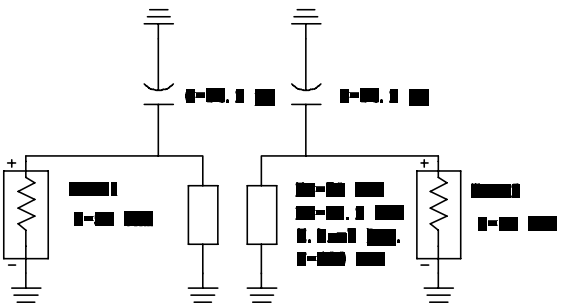

(a)

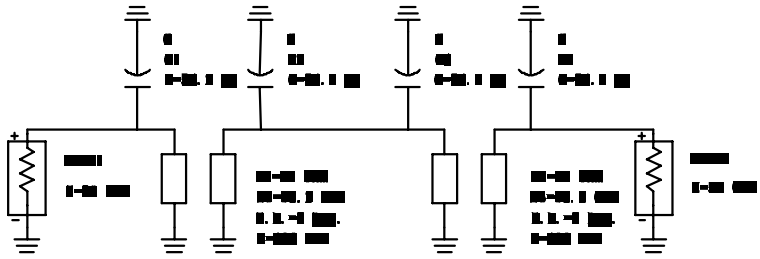

(b)

Fig. 3.3 Model of the proposed one-and two-stage bandpass filter.

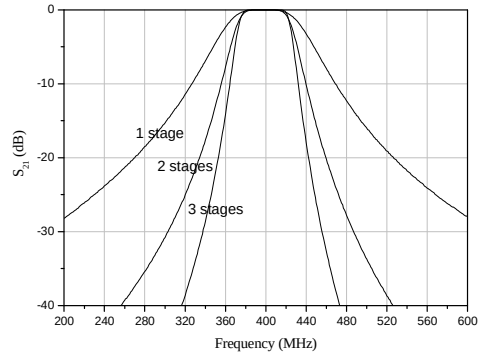

(a)

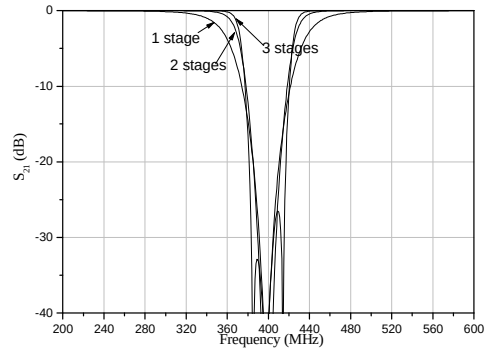

(b)

Fig.3.4 Simulation results of 1, 2 and 3-stage filters for comparison of skirt characteristics: (a) Passband; (b) return loss.

Beside insertion loss, bandwidth is another important parameter of the bandpass filters. There are mainly two factors affecting the bandwidth of the proposed bandpass filter: the electrical length and coupling coefficient of the end shorted coupled lines. Firstly, the bandwidth varies as the electrical length of the coupled lines changes. The longer the length of the coupled lines, the larger the bandwidth is. In Fig.3.5, the quarter-wavelength transmission line has been miniaturized to 1, 2 and 3 degrees and the simulation results of ADS fully proved the correctness of the above discussion. When we miniaturize the quarter-wavelength transmission line, we can choose a proper electrical length according to the bandwidth required.

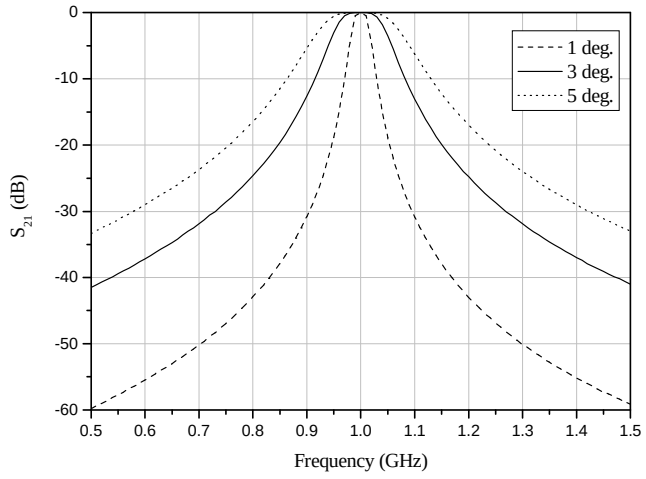

(a)

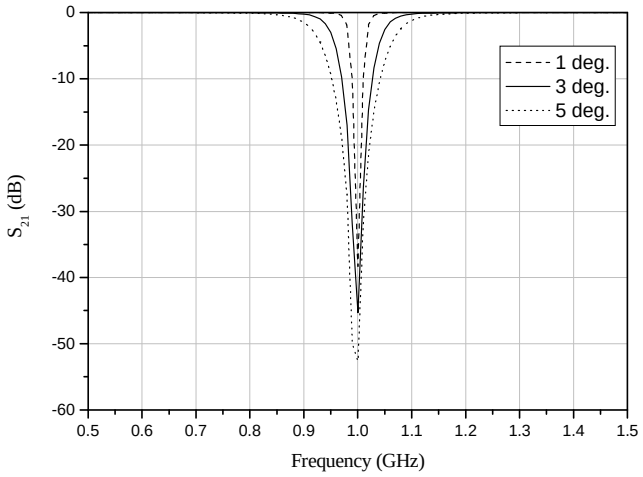

(b)

Fig. 3.5 Different bandwidth according to different electrical length of the coupled lines: (a) Passband; (b) Return loss.

Another factor that affects the bandwidth of miniaturized filter is the coupling coefficient of the coupled lines. To prove this point, let's first check the phase variation of the S_{21} parameter of the miniaturized quarter-wavelength transmission line, which is given here as:

$$S_{21} = \frac{-y_{21}Y_0}{D_Y}.(-1) \tag{3.2}$$

Where

$$\Delta y = (y_{11} + Y_0)(y_{22} + Y_0) - y_{12}y_{21}$$

$$y_{11} = y_{22} = -jY_{0e}\cot\theta - j\frac{Y_{0o}-Y_{0e}}{2}\cot\theta + jB$$

$$y_{21} = y_{12} = -j\frac{Y_{0o}-Y_{0e}}{2}\cot\theta$$

$$B = Y_{0e}\cot\theta + Y_0\cot\theta \qquad (3.3)$$

$$Y_0 = \frac{Y_{0o}-Y_{0e}}{2}$$

Y_{0o}, Y_{0e} are the odd and even mode admittance of the coupled lines respectively.

In equation (3.2), the minus value in the parentheses shows the 180° phase difference between the original quarter-wavelength transmission line and its equivalent miniaturized circuit, which was introduced when we equated the PI network to the end shorted coupled lines. $y_{11}, y_{22}, y_{21}, y_{12}$ are the y-parameters of the equivalent circuit of the quarter-wavelength transmission line. At resonance frequency, equation (3.3) is satisfied when the characteristic admittance Y_{0e} of the end shorted coupled lines is equal to that of the shunt capacitance. With a straightforward analytical manipulation, the equation for the phase of S_{21} can be derived as

Phase of $$S_{21} = \frac{3}{2}\pi + \tan^{-1}x_1 + \tan^{-1}x_2 \qquad (3.4)$$

$$x_1 = \frac{B}{Y_0} - 2\cot\theta - \frac{Y_{0e}\cot\theta}{Y_0} \qquad (3.5)$$

$$x_2 = \frac{B - Y_{0e}\cot\theta}{Y_0} \qquad (3.6)$$

Near the center frequency, x_1 x_2 are expressed by $-\cot\theta$ and $\cot\theta$, respectively, using (3.3). The phase of S_{21} is -90° at the resonance frequency. If the frequency deviates from the center frequency, the relation $C_0\omega = Y_{0e}\cot\theta$ can not be satisfied and the phase of S_{21} starts to deviate from -90°. At this point, the most important item is to decrease the frequency sensitivity of the equivalent $\lambda/4$ transmission line. If Y_{0e} is small, the frequency sensitivity decreases because of the very small shunt value of $C_0\omega$ in the artificial resonance circuit. The coupling coefficient K is:

$$K = \frac{Y_{0o} - Y_{0e}}{Y_{0o} + Y_{0e}} \tag{3.7}$$

From (3.7), the following relation is obtained:

$$Y_{0e} = \frac{1-K}{1+K} Y_{0o} \tag{3.8}$$

In (3.8), when the coupling coefficient is nearly unity, Y_{0e} is very small. The 90° phase shift near the center frequency is independent of the coupling coefficient K. The larger the coupling coefficient K, the broader the bandwidth of the bandpass filter, as illustrated by Fig. 3.6, where the electrical length of the coupled lines is chosen as 7 º and two stages are used.

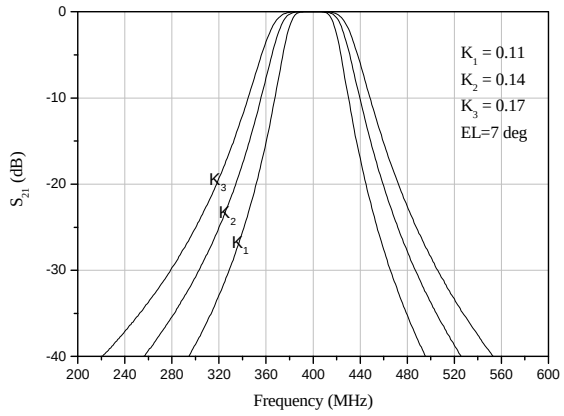

(a)

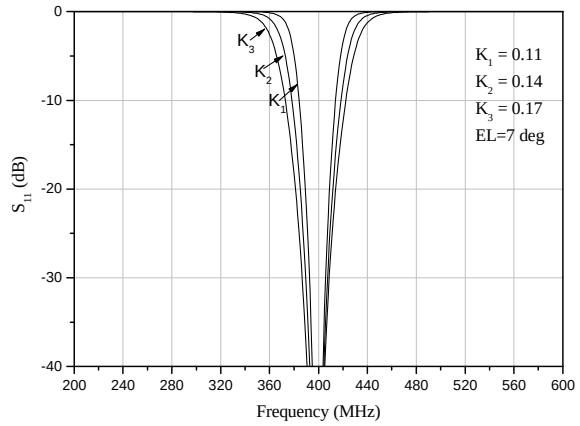

(b)

Fig.3.6 Relation between the bandwidth and coupling coefficient of the coupled lines: (a) Passband and (b) Return loss.

The proposed miniaturized filter is a kind of comb-line filter, but is different from the traditional one mentioned in the introduction part of this paper. Before concluding the design theory of the bandpass filter,

a comparison is made here between the proposed comb-line filter and the traditional one.

Firstly, an inter-stage microstrip transmission line is used between two resonators (stages) in the modified comb-line filter to prevent the unwanted coupling between the neighboring two resonators. At the same time, the insertion of the short transmission line does not affect the active characteristics of the modified bandpass filter.

Secondly, there are resonance circuits at both the input and output ports. In a traditional comb-line filter, the end shorted transmission lines used as input and output are equivalent to shunt inductors. A very small length of the input and output transmission line will lead to a very small inductance and therefore an extremely large impedance, and the input signal will not be able to flow at all. This has hindered the miniaturization of the traditional comb-line filter. Usually the length of transmission lines in the traditional comb-line filter is about $\lambda/8$. However, in the modified one, the problem is solved with the resonant structure used at both the input and output ports. At the same time, two more poles are added because of the added resonant circuits, which contribute to the sharp shirt characteristics of the modified com-line filter.

Finally, the size of the modified comb-line filter can be extremely miniaturized according to $Z^{'} = \dfrac{2Z_{0e}Z_{0o}}{Z_{0e} - Z_{0o}}$, whose potential has been neglected in traditional comb-line filters. For a given Z_0, the electrical length of the parallel coupled lines can be made very small, so long as we choose $Z_{0e} \approx Z_{0o}$.

Chapter 4 Fabrication and Measurement

4.1 EM simulation using HFSS

The theoretical values calculated through the deduced equations have been confirmed through ADS simulation. And the width and length of each transmission line can be obtained by ADS Line Calculation Tool. However, the ADS simulation and calculation are carried out in ideal cases, which have not taken into consideration many potential factors that may affect the performances of the filter. At the same time, two very sensitive composing pars of this filter, capacitors and the inter-stage connecting lines must be studied as they will be proved to be very sensitive in this designed circuit. For the above reasons, we utilized an electromagnetic simulator Ansoft HFSS to simulate the designed filter before fabrication. On the one hand we can get to know the different parts that affect the performances of the whole circuit, and on the other hand we can save both the fabrication cost and time.

HFSS is the industry-standard software for S-parameter and full-wave SPICE extraction and for the electromagnetic simulation of high-frequency and high-speed components. The model of the proposed filter in HFSS is offered here in Fig.4.1. MIM capacitor is used as the model of lumped capacitors, because the exact equivalent circuit of lumped capacitor is unknown.

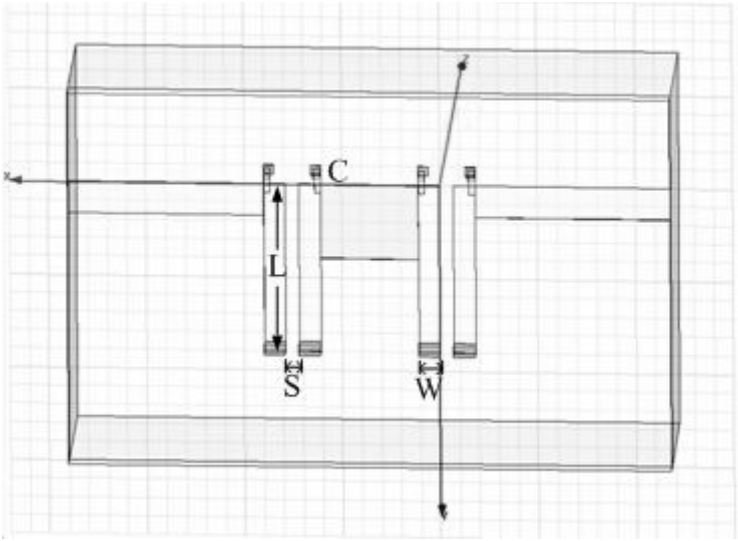

Fig. 4.1 Model of the designed filter in HFSS with MIM capacitors being used.

A bandpass filter working at 400 MHz was designed to confirm the theories in the above chapters. According to (2.9), the capacitor value is calculated to be 54 pF. However, in simulation, the use of 54 pF MIM capacitor has shifted the center frequency from the predicted 400 MHz to 350 MHz, as illustrated in Fig.4.2. Here, by reducing the capacitor value to 45 pF, the center frequency of the designed filter can be moved back to 400 MHz. So capacitors of 45 pF should be used to achieve a proper center frequency, instead of the theoretical 45 pF. As a rule of thumbs, the midband of the proposed modified bandpass filter increases as the capacitor value decreases, and vice versa. The dotted line given in Fig.4.2 is the result of using 36 pF

capacitors in the designed bandpass filter, which leads to a 450 MHz midband.

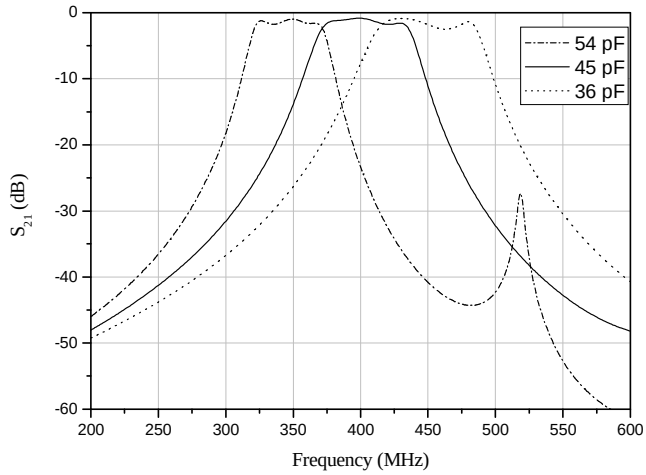

(a)

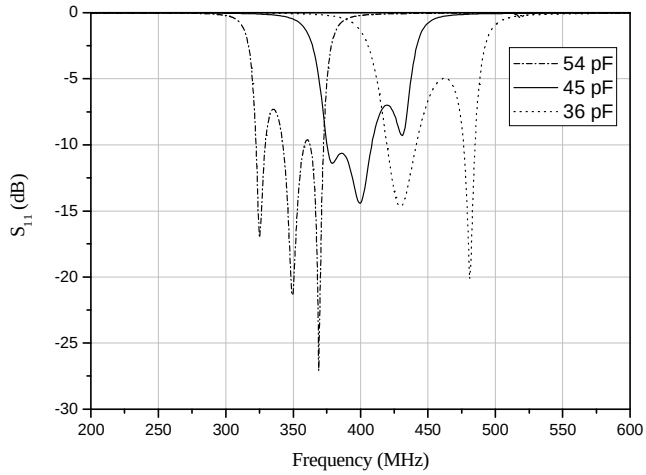

(b)

Fig. 4.2 The relation between lumped capacitor value and center frequency of the bandpass filter: (a) insertion loss; (b) return loss.

In the following paragraphs, emphasis is laid on checking the functions of the inter-stage connecting transmission line, first the effect of width and then that of the length. First of all, we try several kinds of inter-stage connecting lines with the same length but different widths, With others being the same, different width in the inter-stage connecting line will affect the insertion loss of the filter, as shown in Fig. 4.3. Also, the center frequency may deviate a little from the 400 MHz by a few percent as a result of the different widths. In Fig.4.3, we give the simulated results of HFSS, with the width of the inter-stage connecting line being 1.7 mm, 4.0 mm, and 5.0mm. When a width of 4.0 mm is used, the filter shows the best performances in that of both the insertion loss and center frequency. Therefore, the width of the inter-stage connecting line will be fixed at 4.0 mm in the following simulation work where the length of the connecting line is changed.

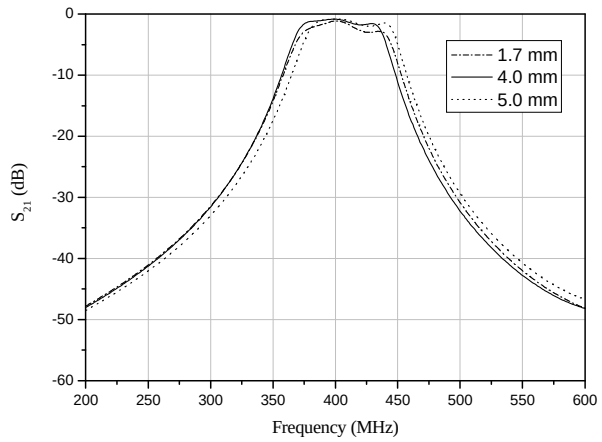

Fig. 4.3 The insertion loss performances according to three kinds of inter-stage connecting lines with different widths.

The next step is to change the length of the inter-stage connecting line until a proper length value that optimizes the performances of the bandpass filter is found. Since this filter has been focusing on a miniaturized size, the inter-stage transmission line between two stages should also made be as small as possible. Therefore, we start our simulation from a length of 1 mm, but the S_{21} performance has been surprisingly bad with the inter-stage connecting line being 1 mm. When the length is increased, S_{21} gets better. Fig.4.4. lists the insertion loss performances according to HFSS simulation, where the length of the inter-stage connection line has been made from 1 mm to 6mm. From the figure, it is easy to find that in this bandpass filter the middle connecting transmission line must be longer than 2 mm for a good insertion loss. Here 5 mm is used, at which both the center frequency and insertion has turned to be satisfactory. Longer lengths will result in a large circuit area and yet not tried in this work.

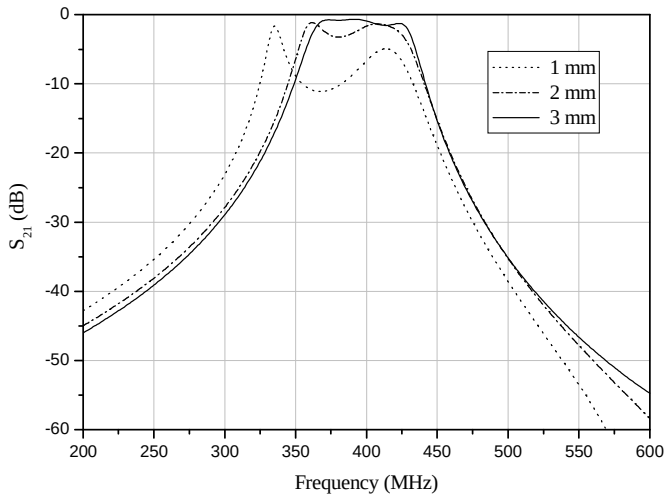

(a)

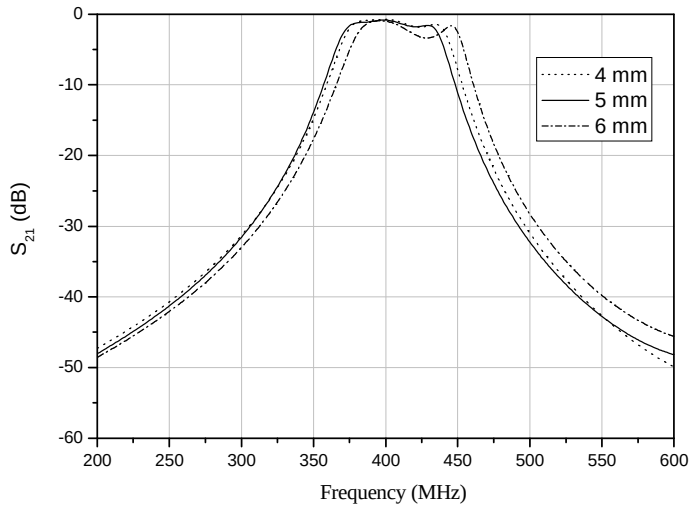

(b)

Fig. 4.4 The insertion loss performances according to different lengths in the inter-stage connecting transmission line.

HFSS simulation is necessary in our work before fabrication is carried out. In the above discussed 400 MHZ bandpass filter we employ HFSS to find the proper capacitor value, the optimum length and width of the inter-stage connecting line. To design a different bandpass filter of this type that working at a different midband or with a different bandwidth, this kind of simulation work is strongly recommended.

4.2 Fabrication and Measurement

Now each design parameter of this 400 MHz bandpass filter has been calculated and optimized in the above section. Here it is summarized in Table 4.1. The layout of the filter used in fabrication that was drawn through Microsoft Visio is given here in Fig.4.5 (a), with the size of the circuit area being 18 mm by 9 mm. A comparison of the sizes of different types of compact filters is made here, as illustrated in Table 4.2. A photograph of the fabricated filter is available in Fig.4.5 (b).

Table 4.1 Design parameters of the fabricated circuits

Parameters	Value (unit)
Thickness of PCB	0.762 mm
Dielectric constant of PCB	3.5
Midband	400 MHz
Electrical length of Coupled lines	7 degree
Length of coupled lines	9.0 mm
Slot of coupled lines	0.7 mm
Width of each coupled lines	1.1 mm
Z_{0o}	70 Ohm
Z_{0e}	52 Ohm

Width of Connecting line	4 mm
Length of connecting line	5 mm
Lumped capacitor value	45 pF
Port impedance	50 Ohm

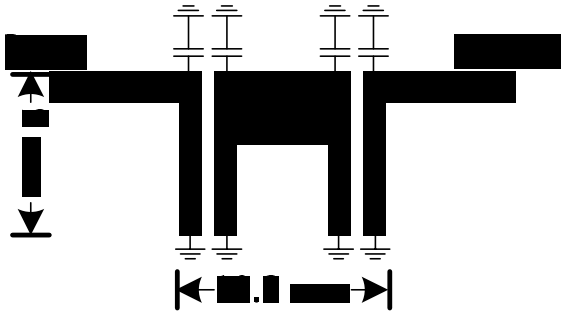

(a)

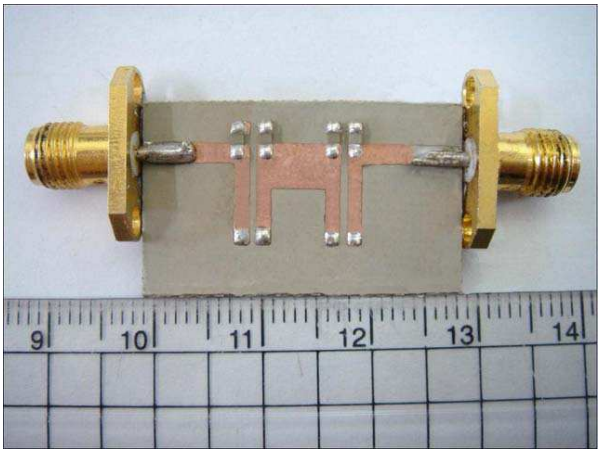

(b)

Fig 4.5 The layout (a) and photo (b) of the designed two-stage bandpass filter centered at 400 MHz.

Table 4.2 Comparison of the sizes of different compact bandpass filters (one resonator).

Type	Author	f_0 (MHz)	Er	E.L.	Physical size (mm^2)
Slow-wave	Jiasheng Hong	1335	10.8	85	16*6.5
SIR	Makimoto	1000	2.6	141	71*5.5
Ceramic Combline	Huiwen Yao	915	38.2	45	3.0*3.0
Proposed	In-ho Kang	400	3.56	7	9*2.9

E.L.: The electrical length of a resonator in degree.

Er: The dielectric of the PCB used for fabrication.

The measurement of the fabricated filter was done with the HP network analyzer. Fig.4.6 compares HFSS simulated results and measured results. And some detailed performances of the bandpass filter are offered in Table 4.3. The measured center frequency is shifted from 400 MHz to the left by 15 MHz due to the difference between MIM and lumped capacitors. Although HFSS has been employed to find the proper capacitor value in the previous work, it is MIM capacitor that was used in the HFSS model used for simulation. Capacitance of the lumped capacitor available in the lab is a little different from that of the MIM capacitor, leading to a deviated center frequency. The spurious passband has been well suppressed and not

observed even up to 10 GHz, as shown in Fig.4.7. Please refer to chapter 1 for the reason of the very wide upper stopband.

Table 4.3 Characteristics of the Fabricated Bandpass Filter.

Midband (MHZ)	385
Pass band (MHZ)	360 to 410
Insertion Loss (dB)	-3.1 at f_0
Attenuation (dB)	-57 at $2 f_0$, -55 at $3 f_0$
Ripple	0.9 dB
Port Impedance	50 Ohm

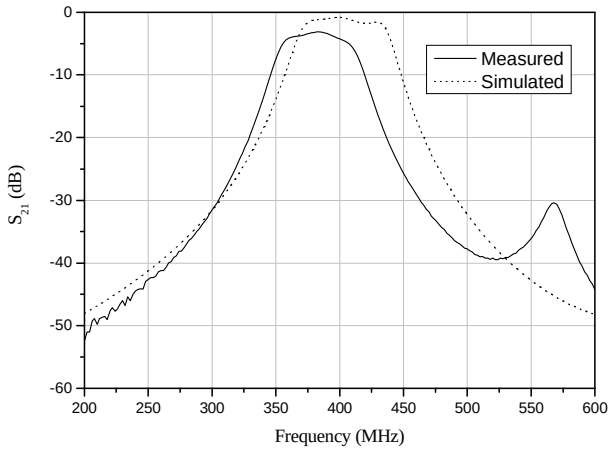

(a)

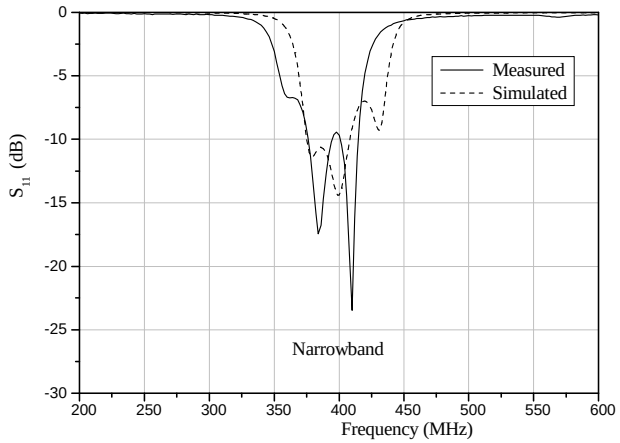

(b)

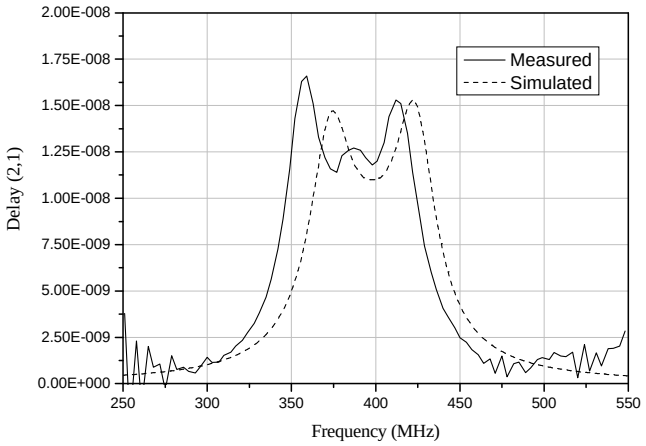

(c)

Fig.4.6 Comparison of simulated and measured results: (a) Insertion loss; (b) Return loss; (c) Group delay.

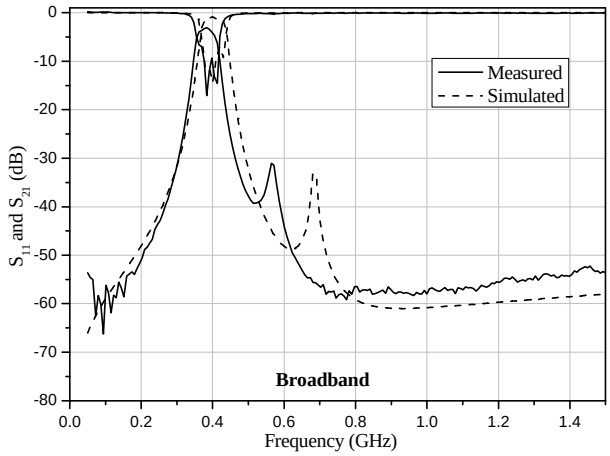

Fig. 4.7 A broadband performance of the bandpass filter to show the suppression of the spurious passband.

Chapter 5 Conclusion

In this thesis, a novel comb-line filter is successfully developed using coupled line structure. Compared with the traditional comb-line filter, the proposed filter takes up a much smaller circuit area. This is because the electrical length of the coupled lines that determines the size of comb-line filters can be reduced to just a few degrees, with the help of lumped capacitors. The suppression of the spurious passband is another advantage of the modified comb-line filter. The spurious passband was not observed up to 10 GHz. Measured results of the fabricated 400MHz filter matched very well with the simulated performances, which verified the validity of the size-reduction method. This size-reducing concept can also be extended to the MMIC field.

References

[1] M. Makimoto and S. Yamashita, “Bandpass filters using parallel coupled strip-line stepped impedance resonators,” *IEEE Trans. Microwave Theory Tech.*, vol. MTT-28, NO. 12, pp. 1413–1417, Dec.1980.

[2] J. S. Hong and M.J. Lancaster, “Theory and experiment of novel microstrip slow-wave open-loop resonator filters,” *IEEE Trans. Microwave Theory Tech.*, vol. 45, NO. 12, pp. 2358–2365, Dec.1997.

[3] G. L. Matthaei, “Comb-line band-pass filters of narrow or moderate bandwidth,” Microwave Journal, vol.6, pp.82-91, Aug. 1963.

[4] Tetsuo Hirota, Akira Minakawa, “Reduced-size branch-line and rat-race hybrids for uniplanar MMIC’s,” *IEEE Trasns. Microwave Theory Tech.*, Vol.38, No. 3, March 1990

[5] P. Vizmuller, *RF Design Guide*, Artech House Inc., Norwood, MA 1995, pp. 219-220.

[6] B.Piernas, K.Nishikawa,T.nakagawa and K. Araki, “Iproved tree-dimensional GaAs inductors,” *IEEE MTT-S International Microwave Smposium Digest*, 2001, pp. 189-192

[7] L.H.Lu, P.Bhattacharya and L.P.B. Katehi, “X-band and K-band lumped Wilkinson power dividers with micromachined technology,” *IEEE MTT-S International Microwave Symposium Digest*, 2000,pp.287-290.

[8] X.Huo, K.J. Chen and P.C.H Chan, “High Q copper inductors on standard silicon substrate with a low K BCB dielectric layer,” *IEEE MTT-S International Microwave Smposium Digest*, 2002, pp.513-516

[9] R.K. Gupta and W.J. Gestinger. “Quasi-lumped-element 3-and 4-part networks for MIC and MMIC applications,” *IEEE MTT-S International Microwave Smposium Digest,*1984, pp.409-411.

[10] G. Matthaei, L. Young and E.M.T. Jones, *Microwave Filters, Impedance Matching Networks and Coupling Structures*, Artech House Inc., Norwood, MA 1980, p.220

[11] G. Matthaei, L. Young and E.M.T. Jones, *Microwave Filters, Impedance Matching Networks and Coupling Structures*, Artech House Inc., Norwood, MA 1980, p. 433.

Acknowledgement

I would like to deliver my sincere thanks to many people who have offered me enormous help in both my study and daily life during the past two years. Had it not for their generous supports, it would have been an impossible task for me to finish my two years' study, let alone my dissertation.

I will never be able to thank enough my mentor, Professor In-ho Kang, a great professor and an intelligent scholar. In fact, the word thanks can hardly express my so much gratitude to him for the each and every thing he has done for my account. His wide knowledge, strict research attitude and enthusiasm in work have already influenced my way to think and to study. His optimism facing the emerging academic problems has taught me how to deal with the problems that will come out in my future research work.

I am very grateful to Professor Dongkook Park in the Department of Electronic and Communication Engineering for the trouble he has taken to deliver English lectures to us. I am also thankful to the other Professors of our department for their supports and guidance on this work, who are Professor Young Yun, Professor Dong Il Kim, Professor Kyeong-Sik Min, Professor Hyung Rae Cho, Professor Ki Man Kim, Professor Ji Won Jung.

I want to say thanks to my senior Mr. Li Rui. His help to me had started even before my stepping on the land of Korea. Certainly, I cannot be thankful enough to our laboratory members, Miss Haiyan Xu and Mr. Shiwei Shan for their timely and unselfish help. They not only help me with my research work, but also let me enjoy the friendly work environment. My heartfelt thanks are also due to the friends in Microwave and Antenna lab, Mr. Han Tea kyoung, Mr. Seo Yong Gun and others who offered me great helps in my experiments.

Finally, I would like to express my sincere thanks to Professor Yingji Piao and Mr. Zheng Li at Qingdao University of China. Without their recommendation, it is impossible for me to get the opportunity to study in Korea.